Spectroscopic and Structural Investigation of the Confinement of D and L Dimethyl Tartrate in Lecithin Reverse Micelles

Sergio Abbate,[†,‡,▽] Franca Castiglione,[||,▽] France Lebon,[†,‡,▽] Giovanna Longhi,[†,‡,▽] Alessandro Longo,[⊥,▽] Andrea Mele,[||,#,▽] Walter Panzeri,[#,▽] Angela Ruggirello,[§,▽] and Vincenzo Turco Liveri*[,§]

Dipartimento di Scienze Biomediche e Biotecnologie, Università di Brescia, Viale Europa 11, 25123, Brescia, Italy, Consorzio Nazionale Interuniversitario per le Scienze Fisiche della Materia (CNISM), Via della Vasca Navale, 84 - 00146 Roma, Italy, Dipartimento di Chimica Fisica, Università di Palermo, Viale delle Scienze, Parco d'Orleans II, 90128, Palermo, Italy, Dipartimento di Chimica, Materiali e Ing. Chimica, "Giulio Natta" Politecnico di Milano, Via L. Mancinelli, 7 - 20131 Milano, Italy, ISMN, Istituto per lo Studio dei Materiali Nanostrutturati, CNR, Via U. La Malfa 153, 90146 Palermo, Italy, and ICRM, Instituto di Chimica del Riconoscimento Molecolare, CNR, Via L. Mancinelli, 7-20131 Milano, Italy

Received: November 6, 2008; Revised Manuscript Received: December 23, 2008

The confinement of D and L dimethyl tartrate in lecithin reverse micelles dispersed in cyclohexane has been investigated by FT-IR, polarimetry, electronic and vibrational circular dichroism (ECD and VCD), ^{1}H NMR, and small-angle X-ray scattering (SAXS). Measurements have been performed at room temperature as a function of the solubilizate-to-surfactant molar ratio (R) at fixed lecithin concentration. The analysis of experimental data indicates that the dimethyl tartrate molecules are solubilized within reverse micelles in proximity to the surfactant head groups in the same way for the D and L forms. The encapsulation of dimethyl tatrate within lecithin reverse micelles involves changes in its H-bonds, from what is observed in the pure solid or in CCl_4 solutions; this is a consequence of the establishment of specific solute-surfactant headgroup interactions and of confinement effects. In the $0 \leq R \leq 1.7$ range, SAXS profiles of dimethyl tartrate/lecithin/cyclohexane micellar solutions are well-described by a model of interacting polydisperse spherical micellar cores whose mean radius does not change appreciably with R (i.e., it changes from about 18 to 20 Å). ^{1}H NMR diffusion measurements of both dimethyl tartrates and lecithin were rationalized in terms of collective translational motions of the entire micellar aggregate and of their molecular diffusion among clusters of reverse micelles. The association of optically active lecithin with D and L dimethyl tartrate leads to the formation of self-organized supramolecular aggregates whose interesting chiroptical features are evidenced by polarimetry and CD.

1. Introduction

Soybean lecithin (Epikuron 200) is a purified diacyl phosphatidylcholine mixture of natural origin. The molecular structure of its main component, shown in Figure 1, is characterized by a zwitterionic headgroup (a positively charged choline, a negatively charged phosphate group attached to a glycerol moiety) and two long hydrocarbon chains. Lecithin occurs in many biological systems (membranes, animal tissues, and organs), and its role in nature is strictly connected to the presence of a stereogenic carbon atom (C7) in the glycerol moiety and to the coexistence of spatially separated polar and apolar domains, leading to self-assemble capability and formation of ordered chiral nanostructures both in aqueous and in apolar media. For these reasons, lecithins are considered of utmost importance to model or mime some aspects of cell membranes.[1,2]

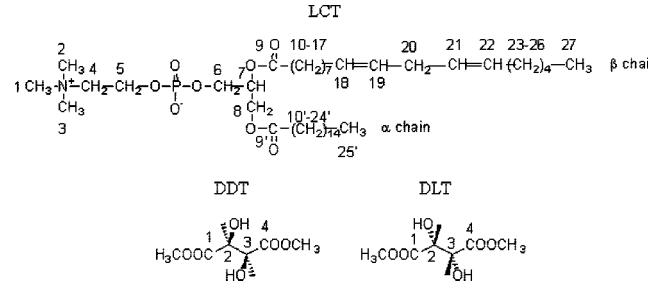

Figure 1. Molecular structure and atom numbering of the main component of lecithin (LCT), dimethyl D-tartrate (DDT) and dimethyl L-tartrate (DLT).

Among all possible molecular aggregates formed by lecithin when dissolved in polar or apolar solvents, reverse micelles are of particular interest.[3−5] These dynamic molecular assemblies are constituted by a micellar core of opportunely arranged surfactant zwitterionic heads surrounded by the hydrophobic layer formed by the alkyl chains. The main property of these peculiar aggregates is the ability to incorporate a large variety of solubilizates in their interior. Either polar or ionic species are entrapped in the micellar core and dispersed among the

* Corresponding author. Fax: 0039 091 590015. Tel: 0039 091 6459844. E-mail: turco@unipa.it.
† Università di Brescia.
‡ CNISM.
§ Università di Palermo.
|| "Giulio Natta" Politecnico di Milano.
⊥ ISMN.
ICRM.
▽ E-mail: S.A., abbate@.unibs.it; F.C., franca.castiglione@chem.polimi.it; F.L., lebon@.unibs.it; G.L., longhi@med.unibs.it; A.L., alex@pa.ismn.cnr.it; A.M., andrea.mele@polimi.it; W.P., walter.panzeri@icrm.cnr.it; A.R., a.ruggirello@unipa.it; turco@unipa.it.

10.1021/jp809793u CCC: $40.75
Published on Web 02/17/2009

surfactant head groups or they form well-defined clusters; amphiphilic molecules are preferentially solubilized, opportunely oriented, in the palisade layer (the monolayer comprising the surfactant head groups and the alkyl chains); and finally apolar substances are mainly dispersed in the bulk solvent medium.[6]

However, the specific location of the solubilizate depends not only on its structural features[7] but also on the lecithin concentration; the apolar solvent type strongly influences the hosting capability of the micellar aggregates.[8−10] In principle, the properties of confined substances within reverse micelles are different from those of isolated molecules or of molecules in the pure bulk state; these properties can be opportunely modulated by changing some external parameters as the solubilizate to surfactant molar ratio (R), the temperature and the surfactant concentration.[11] In particular, solubilization of chiral molecules within such aggregates could be used to stabilize specific conformations.

Among tartaric acid derivatives, dialkyl tartrates have wide applications, in particular, in organic and pharmaceutical chemistry as catalysts for asymmetric synthesis and as chiral intermediates. It has been reported that dialkyl tartrates can exist in different conformations and interaction with the solvent affects the predominant one.[12]

In a previous investigation we reported on the solubilization of D and L dimethyl tartrates (see Figure 1 for molecular structures, atom numbering, and absolute configurations) in sodium bis(2-ethylhexyl)sulfosuccinate (AOT) reverse micelles dispersed in carbon tetrachloride. In that case, the analysis of FT-IR and vibrational circular dichroism (VCD) spectra led to hypothesize that both enantiomers are entrapped within reverse micelles driven by the establishment of specific interactions with surfactant head groups.[13]

In the present contribution we want to extend that study to the confinement of D and L dimethyl tartrates in lecithin reverse micelles to clarify the influence of the surfactant nature on the state of dimethyl tartrates and to put into evidence similarities and differences.

The specific confinement effects have been investigated by FT-IR, polarimetry, VCD and ECD (vibrational and electronic circular dichroism), and ^{1}H NMR spectroscopies, whereas structural information concerning the resulting chiral molecular assemblies has been gained by small-angle X-ray scattering (SAXS). The choice of cyclohexane as apolar solvent over previously used carbon tetrachloride was made because the latter solvent is opaque to X-rays; also UV−CD experiments are not limited at shorter wavelengths.

2. Materials and Methods

(−)-(2*S*,3*S*)-Dimethyl tartrate (dimethyl D-tartrate or DDT, Fluka, optical purity >99%), (+)-(2*R*,3*R*)-Dimethyl tartrate (dimethyl L-tartrate or DLT, Fluka, optical purity >99%), cyclohexane (Aldrich, 99+%, ACS reagent) and cyclohexane-d_{12} (Cambridge Isotope Laboratories Inc., D 99.5%) were used without further purification. Soybean phosphatidylcholine (lecithin or LCT, Degussa, Epikuron-200, generous gift of Degussa Texturan Systems) was dried under vacuum for several days before use. According to the producer, this substance contains more than 95% of phosphatidylcholine (PC).

Solutions at various solubilizate-to-surfactant molar ratios (R) were prepared by adding the appropriate amounts of LCT/C_6H_{12} and LCT/C_6D_{12} solutions to weighed quantities of DDT or DLT. To remove residual traces of water, solutions of DDT and DLT in lecithin/C_6H_{12} and lecithin/C_6D_{12} were gently stirred for several days in the presence of activated type 4A molecular sieves (Fluka, beads of 4 Å pore size). Deuterated solvents were used for FT-IR, NMR, VCD, and ECD (in the latter case not necessary). Undeuterated solvents were used for polarimetry and SAXS. According to literature, we assumed that the isotopic substitution does not involve significant changes in the micellar properties.[14]

Though dimethyl D-tartrate and dimethyl L-tartrate are scarcely soluble in pure C_6H_{12}, in a 0.08 M solution of lecithin/C_6H_{12} and lecithin/C_6D_{12}, the highest concentration, expressed a tartrate-to-lecithin molar ratio (R) of $R = 1.7$ for both tartrates in the presence of solubilizate crystals.

FT-IR spectra is all liquid samples were recorded in the spectral region 900−4000 cm^{-1} using a Perkin-Elmer (Spectrum BX) spectrometer and a cell equipped with CaF_2 windows. The FT-IR spectra of solid D and L dimethyl tartrate were recorded using a pressed disk of the compound mixed with KBr powder. All measurements were collected at room temperature (RT) with a spectral resolution of 2 cm$^{-1.}$

VCD spectra in the mid-IR region were taken in 0.05, 0.1, and 0.2 mm path length BaF_2 cells using a JASCO FVS4000 FTIR instrument equipped with a liquid N_2-cooled MCT detector; 4000 scans were taken, with 4 cm^{-1} resolution. The spectra were recorded at RT for both enantiomers, and mirror image appearance was obtained for them (see the Supporting Information file with the VCD spectra for both enantiomers, wherefrom the VCD spectra of DDT reported in Figures 6 and 8 in the text were derived). The VCD spectra of Figures 6 and 8 are the semidifference of DDT and DLT VCD spectra, i.e., (1/2)(DDT-DLT). ECD spectra in the UV region 185−300 nm were taken in a 0.1 mm path-length SiO_2 cuvette using a N_2-purged JASCO 815SE apparatus (5 scans, $\tau = 1$ s). The DDT/LCT/C_6D_{12} and DLT/LCT/C_6D_{12} solutions at various R values ($R = 0.5$, 1.5, and 1.7) were diluted 10 times with C_6D_{12}.

Optical rotation measurements have been performed on a JASCO P-1010 polarimeter at the sodium D line and using a 1 dm optical path cell.

Small angle X-ray scattering spectra have been collected at 25 °C with a Nanostar apparatus (Bruker) equipped with a copper anode Cu Kα, Ni filtered ($\lambda = 1.5418$ Å) and a bidimensional detector. The magnitude of the scattering vector (q) is given by $q = 4\pi \sin\theta/\lambda$, where 2θ and λ are the scattering angle and incident X-ray wavelength, respectively. Each scattering spectrum of freshly prepared samples was subtracted by the cell and solvent contributions. Best-fit analyses were performed using the IGOR program.

All the NMR experiments were carried out in C_6D_{12} on a Bruker Avance spectrometer operating at 500 MHz proton frequency. Chemical shifts were referenced to external tetramethylsilane (TMS). Spectral assignments of lecithin were supported by standard two-dimensional correlation methods such as COSY and TOCSY. Two dimensional nuclear Overhauser enhancement correlation experiments (NOESY) were acquired by using standard library pulse sequences. Typical settings: 50 ms mixing time to avoid spin diffusion artifacts, 512 increments in F1 dimension, 16 scans for each F1 increment, 2K data points in F2 dimension. All the spectra were recorded at 298 K.

Diffusion ordered correlation experiments (DOSY) were carried out on a Bruker Avance 500 spectrometer equipped with a pulsed field gradient (PFG) unit capable of producing magnetic field pulse gradients in the z-direction of 53 G cm^{-1}. All the experiments were performed using the bipolar pulse longitudinal eddy current delay (BPPLED) pulse sequence. The duration of the magnetic field pulse gradients (δ) and the diffusion times (Δ) were optimized for each sample to obtain complete

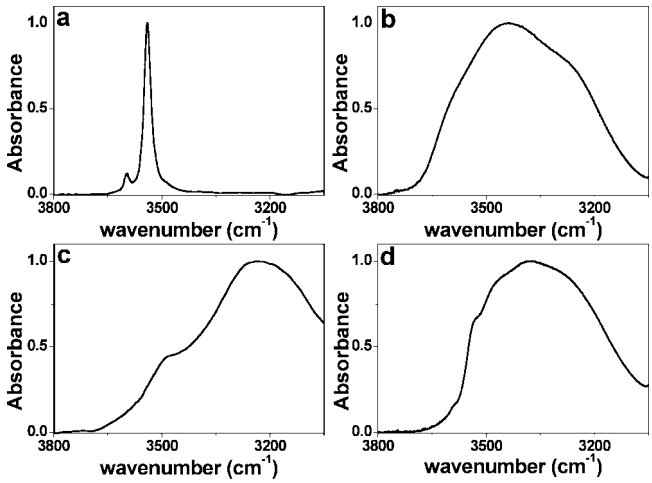

Figure 2. OH stretching band of DDT in CCl_4 solution: [DDT] = 2×10^{-3} M, panel a; solid DDT, panel b; DDT in LCT/C_6D_{12} system at $R = 1.5$, panel c; DDT in AOT/CCl_4 system at $R = 1.5$, panel d.

dephasing of the signals with the maximum gradient strength. Typical values used in this work were $\delta = 4-4.5$ ms and $\Delta = 47-70$ ms. In each PFG NMR experiment, a series of 16 spectra with 32K points were collected. The pulse gradients were incremented from 2 to 95% of the maximum gradient strength in a linear ramp. The temperature was set and controlled at 298 K with an air flow of 535 L h^{-1} to avoid any temperature fluctuations due to sample heating during the magnetic field pulse gradients.

3. Results and Discussion

3.1. Infrared and VCD Measurements. As shown in panel a of Figure 2, when dimethyl D-tartrate is monomerically dispersed in a solution of CCl_4 (we could not use a solution in C_6D_{12}, due to limited solubility of dimethyl tartrate in this solvent), it is characterized by a sharp band centered at 3540 cm^{-1} and a shoulder at 3597 cm^{-1} attributed respectively to the stretching vibration of the OH group intramolecularly bonded to the carbonyl group and to the O-CH_3 moiety.[15,16]

Solubilization of dimethyl D-tartrate in 0.08 M lecithin/cyclohexane solutions, on the other hand, causes marked changes of shape and position of the OH band (see Figure 2, panel c) with respect to those of DDT solubilized in CCl_4 solution, indicating the establishment of strong and specific intermolecular DDT-DDT and DDT-LCT H-bonds. A similar behavior is observed for DLT/LCT/cyclohexane solutions.

As highlighted by the comparison between OH stretching bands of DDT solubilized in LCT/C_6D_{12} and sodium bis(2-ethylhexyl)sulfosuccinate (AOT)/CCl_4 systems, shown in Figure 2 panels c and d, respectively, the OH band shape and position appear as strongly surfactant-dependent, thus indicating the occurrence of specific tartrate−surfactant head groups interactions. In particular, the OH stretching band of DDT solubilized in LCT/C_6D_{12} system is shifted to lower wavenumbers with respect to that of DDT/AOT/CCl_4 solution at the same R value. By comparing also with the solid DDT data (panel b, Figure 2), we deduce that the strength of DDT-LCT headgroup interactions is stronger than that between DDT and AOT head groups.

The R dependence of the OH stretching bands of DDT dissolved in LCT/C_6D_{12} solutions, obtained by subtracting the spectrum of LCT/C_6D_{12} system and normalized such that the band maximum at ca. 3300 cm^{-1} has Absorbance = 1, is shown in Figure 3. For the sake of comparison, the spectra of dimethyl

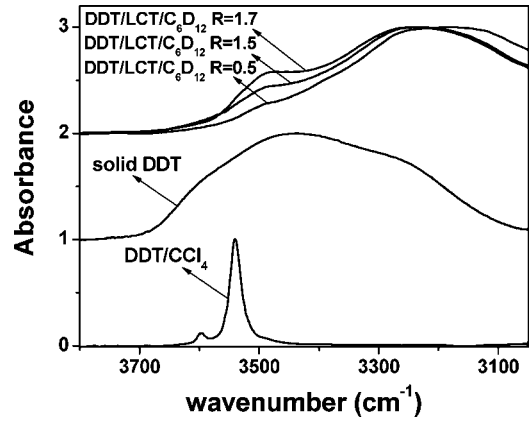

Figure 3. Normalized OH stretching bands of DDT as a pure solid, in CCl_4 solution, and in the DDT/LCT/C_6D_{12} system at various R values.

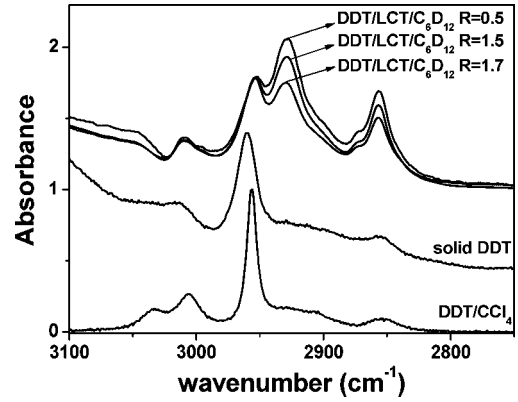

Figure 4. CH stretching bands of DDT in the solid state, in CCl_4 solution, and in LCT/C_6D_{12} solutions.

D-tartrate in the solid state and in CCl_4 solution is also shown. It can be noted that the OH bands are progressively shifted to higher wavenumbers by increasing R and that, notwithstanding this shift, appreciable spectral differences with respect to the band of solid DDT are observed. Moreover, one may note that the contribution of the component centered at about 3485 cm^{-1} increases significantly in relative intensity with R.

The shift to higher wavenumbers of the OH band with increasing R, as already observed in the case of AOT, can be explained considering that, by increasing the amount of DDT, a larger number of tartrate molecules is solubilized per micelle and they are progressively less deeply inserted within reverse micelles thus establishing weaker H-bonds with lecithin head groups. However, the OH band never coincides or does even approach that of pure solid DDT indicating that, even at the highest R value, a well-defined cluster of DDT molecules entrapped within micellar core is not formed.

The CH stretching band of DDT dissolved in LCT/C_6D_{12} solution at various R, obtained by subtracting the spectrum of LCT/C_6D_{12} from that of DDT/LCT/C_6D_{12} and normalizing to the same Absorbance value of the band maximum at about 2950 cm^{-1}, together with the CH band of DDT in the solid state and in solution are shown in Figure 4.

In the spectra of confined DDT one may notice the appearance of additional spectral features with respect to the single band of pure or monomeric DDT, and changes in the relative intensity of these features; this may suggest that the interaction of DDT with reverse micelles involves some variations in the lateral packing order and/or conformational dynamics of CH tartrate

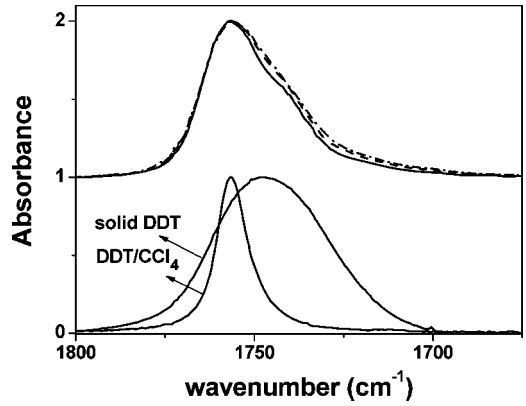

Figure 5. Normalized C═O stretching bands of solid DDT, DDT/CCl_4 ([DDT] = 2×10^{-3} M), and DDT/LCT/C_6D_{12} system at various R values ([LCT] = 0.08 M; R = 0.5, solid line; R = 1.5, dashed line; R = 1.7, dashed-dotted line). (DDT C═O stretching bands of DDT/LCT/C_6D_{12} systems are obtained by subtracting the LCT/C_6D_{12} spectrum from DDT/LCT/C_6D_{12} spectra).

groups and/or lecithin alkyl chains.[17] This effect seems more prominent at lower R values, i.e., when the fraction of tartrate molecules strongly interacting with lecithin head groups is higher.

Figure 5 shows the C═O stretching band of dimethyl D-tartrate solubilized in LCT reverse micelles obtained by subtracting the spectrum of LCT/C_6D_{12} system from those of DDT/LCT/C_6D_{12} solutions. For comparison, the C═O stretching band of dimethyl D-tartrate as a pure solid and in CCl_4 solutions are also displayed. One may note that although DDT dispersed in CCl_4 is characterized by a sharp peak centered at 1757 cm^{-1} and DDT in the solid state is characterized by a broad symmetric band centered at 1748 cm^{-1}, the C═O stretching of confined dimethyl D-tartrate is centered at 1757 cm^{-1} with a shoulder at 1740 cm^{-1}; this finding suggests that the predominant orientation assumed by tartrate molecules when solubilized in lecithin reverse micelles makes the two C═O groups nonequivalent or that two different conformers are highly populated and give C═O absorption bands at different frequencies.

On the other hand, no significant changes in the C═O band shape and positions is evidenced with increasing R, indicating that, independently of the DDT content, the carbonyl groups of DDT experience nearly the same environment.

For the carbonyl region we consider also the VCD spectra in Figure 6, precisely the spectra in the 100 μm cell path length of (a) DDT/CCl_4 ([DDT] = 0.04 M), (b) DDT/DMSO ([DDT] = 0.062 M), (c) DDT/AOT/CCl_4, and (d) DDT/LCT/C_6D_{12}.

The carbonyl VCD signals appear quite sensitive to differing intermolecular interactions (with solvent or surfactant). The VCD spectra recorded for DDT in presence of hydrogen bond acceptors, DMSO, AOT, and lecithin, all exhibit the same (−, +, −) pattern as opposed to the (−, +) couplet observed in the VCD spectra of DDT/CCl_4 solution.

The observation of the difference in the VCD spectra of DDT in DMSO and in CCl_4 was made also in ref 12, where considering the calculated VCD spectra of tartrate−$(DMSO)_2$ clusters led to the conclusion that two principal conformations are populated for DDT in DMSO: the latter give two VCD couplets of opposite sign, which are slightly shifted in frequency one with respect to the other.

On the basis of this interpretation and due to the similarities of VCD spectra of panels b−d of Figure 6, we suggest that tartrate strongly interacts with lecithin polar heads.

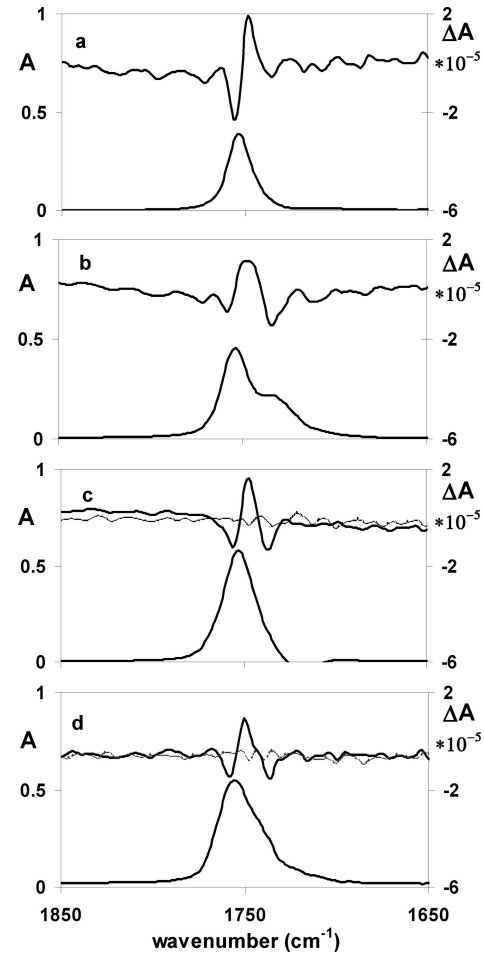

Figure 6. Absorption and VCD spectra (solid line) of (a) DDT/CCl_4 ([DDT] = 0.04 M), (b) DDT/DMSO ([DDT] = 0.062 M), (c) DDT/AOT/CCl_4 ([AOT] = 0.0527 M; R = 2) (AOT/CCl_4 has been subtracted), and (d) DDT/LCT/C_6D_{12} ([LCT] = 0.0395 M; R = 1.7) (LCT/C_6D_{12} has been subtracted). The VCD spectrum of AOT and LCT (solvent has been subtracted) has been presented in panels c and d respectively (dashed line) (see Materials and Methods and Supporting Information).

In conclusion, on the basis of IR and VCD spectroscopy we note that, analogously to what is found in AOT reverse micelles, no significant differences are found for the two enantiomers in LCT reverse micelles.

Parts a and b of Figure 7 show the absorption spectra of DDT in lecithin reverse micelles at various R values, after LCT/C_6D_{12} subtraction, relative to the 1050−1170 and 1150−1370 cm^{-1} spectral regions, respectively. For comparison purpose, the absorption spectra of DDT are shown in CCl_4 solution and in the solid state, normalized such that the maximum absorbance value is 0.1.

The two bands centered at 1135 and 1092 cm^{-1} in the spectrum of solid DDT and at 1125 and 1094 cm^{-1} when DDT is monomerically dispersed in solution have been attributed to modes containing C*−O symmetric and antisymmetric stretchings, respectively.[15,18]

By analyzing the C*−O symmetric and antisymmetric stretching bands of DDT confined in reverse micelles, we can make the following observations: (i) the symmetric C*−O stretching of DDT in LCT/C_6D_{12} is even shifted to higher frequencies with respect to that of DDT dispersed in CCl_4 (1125 cm^{-1}) and even more in the solid state; (ii) the observed shift decreases by increasing R; (iii) even at the highest R, the band

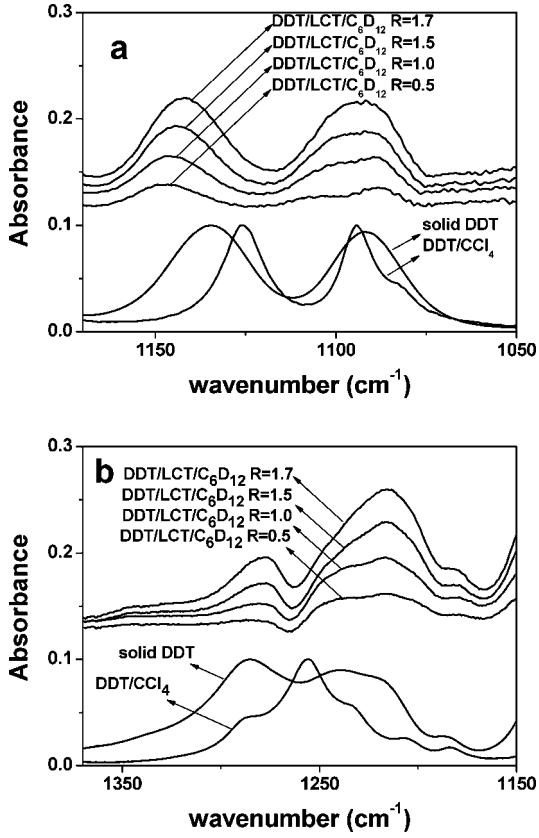

Figure 7. Comparison of absorption spectra of DDT in lecithin reverse micelles at various R values, after LCT/C_6D_{12} subtraction, with that of DDT in CCl_4 solution and in the solid state in the (a) 1050−1170 cm^{-1} and (b) 1150−1370 cm^{-1}spectral regions.

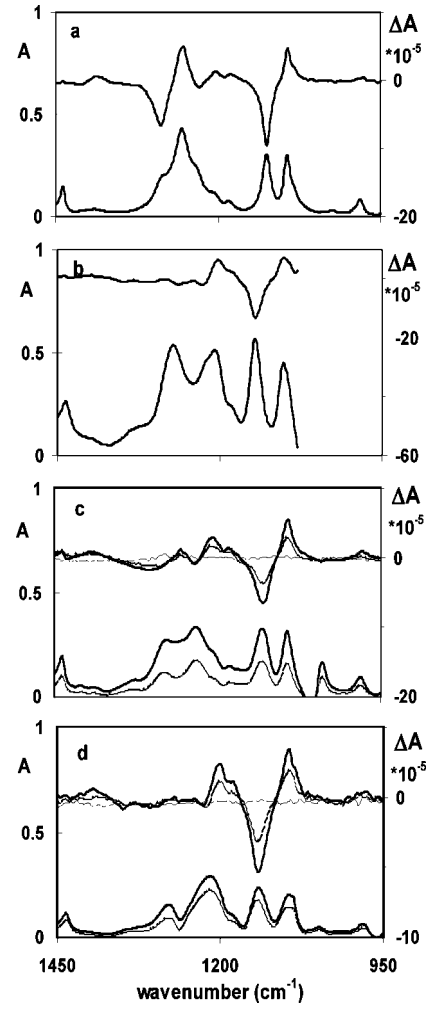

Figure 8. Absorption and VCD spectra of (a) DDT/CCl_4 ([DDT] = 0.04 M), (b) DDT/DMSO ([DDT] = 0.41 M), (c) DDT/AOT/CCl_4 at various R values ([AOT] = 0.158 M; $R = 2$, solid line; $R = 0.7$, dashed line) (AOT/CCl_4 has been subtracted), and (d) DDT/LCT/C_6D_{12} at various R values ([LCT] = 0.08 M; $R = 1.7$, solid line; $R = 1.5$, dashed line) (LCT/C_6D_{12} has been subtracted). The VCD spectrum of AOT and LCT (solvent has been subtracted) has been presented in panels c and d, respectively (dashed-dotted-dotted line) (see Materials and Methods and Supporting Information).

position does not coincide with that of solid; (iv) the antisymmetric stretching band shows some shape changes with R, suggesting the presence of at least two components whose relative contributions are R dependent.

These observations have led us to hypothesize that the DDT−lecithin headgroup interactions are stronger than the DDT−DDT ones and that these interactions are more evident for the first tartrate molecules, which are most deeply inserted within the reverse micelles. The typical situation for solid DDT is approached by increasing R, because less favorable solubilization sites are left for the next tartrate molecules. On the other hand, the occurrence of two components in the antisymmetric stretching band could indicate that the predominant orientation assumed by solubilized molecules leads to unequivalent C*−O moieties.

Considering the band occurring in the 1150−1370 cm^{-1} spectral region (Figure 7b), the higher frequency component is attributed to bending of HC*O and C*OH moieties of the two HC*OH groups; the lower frequency one is instead quite delocalized and is attributed to C−C/C−O stretchings of the $COOCH_3$ groups plus deformations of C*H and OH of the two central groups HC*OH.[15,18]

It is worth noting that this band is quite different from that of DDT in solution and in the solid; further, the two components show a small but definite shift to lower wavenumbers with R, along with the obvious increase in intensity. This reveals the peculiar environment experienced by DDT within lecithin reverse micelles and, in particular, the occurrence of specific DDT−lecithin headgroup interactions whose strength changes with R. However, because the lecithin PO_4^- group shows an absorption band in the same spectral region (1262 cm^{-1}), contributions due to variations in this bands should also be considered.

Also VCD spectroscopy in the mid-IR region appears to be quite sensitive to tartrate−LCT interactions: Figure 8 provides the results, in the 950−1400 cm^{-1} spectral range, for DDT in CCl_4, DMSO, and AOT/CCl_4, reported previously,[13] together with the corresponding new results for DDT in lecithin/C_6D_{12}.

The VCD spectra of DDT in both AOT and lecithin resemble the one recorded in DMSO solution showing a dramatic change with respect to the VCD spectra taken for DDT in a dilute homogeneous solution in an apolar solvent like CCl_4. The most relevant change regards the VCD couplet 1257−1290 cm^{-1} observed in CCl_4 that nearly disappears in AOT micelles, and completely disappears in lecithin complex and in DMSO solution. Also the corresponding IR signals dramatically change, showing an increase in absorption at 1240 cm^{-1} in AOT/CCl_4, at 1220 cm^{-1} in LCT/C_6D_{12} and at 1204 cm^{-1} in DMSO; corresponding with this absorption feature, a positive VCD band is observed at 1204 cm^{-1} both in LCT/C_6D_{12} and in DMSO.

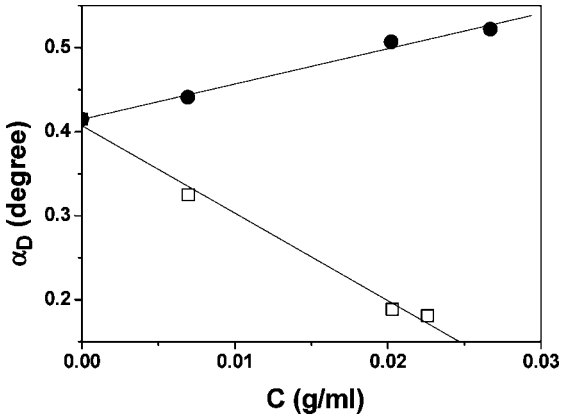

Figure 9. Observed optical rotation (α_D) at the sodium D line of DDT/LCT/C_6H_{12} and DLT/LCT/C_6H_{12} ([LCT] = 0.08 M) measured in a 1 dm cell as a function of respective enantiomers' concentrations (*C*).

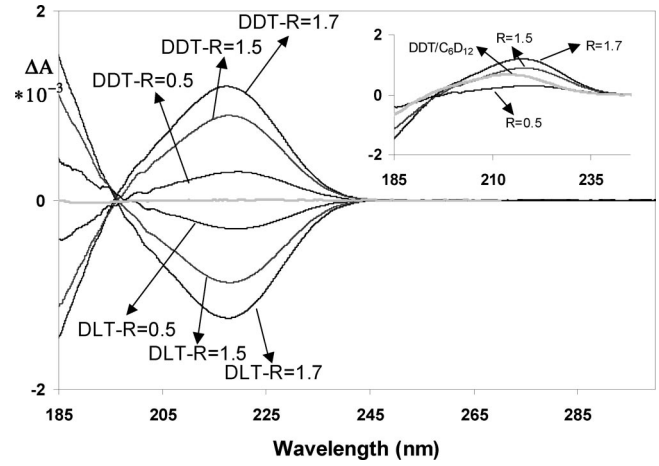

Figure 10. ECD spectra of DDT/LCT/C_6D_{12} and DLT/LCT/C_6D_{12} at various *R* values ($R = 0.5$; $R = 1.5$; $R = 1.7$). Inset: ECD spectra of DDT/LCT/C_6D_{12} at various *R* and DDT in C_6D_{12} (the DDT/C_6D_{12} spectrum has been multiplied by 2 so as to provide easier comparison).

An effect is noticed also for the (+, −) couplet at ca. 1140 and 1100 cm^{-1} and the two corresponding IR bands of equal intensity, assigned to C*O symmetric stretchings (higher frequency) and antisymmetric stretchings (lower frequency) modes, respectively: an evident progressive shift toward higher wavenumbers is noticed in going from CCl_4 (1126 cm^{-1}) to DDT/AOT/CCl_4 (1133 cm^{-1}) to DDT/lecithin/C_6D_{12} (1144 cm^{-1}) finally to DDT/DMSO (1147 cm^{-1}).

The spectroscopic changes observed in the two solutions, CCl_4 and DMSO, have been recently accounted for by DFT calculations in ref 12. They have been related to conformational changes caused by interaction of tartrate with hydrogen bond acceptor S═O groups, suggesting that a change in the dielectric constant experienced by tartrate is not sufficient to explain the experimental results, and intermolecular hydrogen bond formation must be invoked.

For these reasons, as pointed out earlier, the spectroscopic observations regarding the micellar systems are a clear indication of a specific intermolecular[13] interaction of tartrate with surfactant polar heads, either the SO_3^- or PO_4^- group.

3.2. Chiroptical Measurements. The observed optical rotation (α_D) of DDT/LCT/C_6H_{12} and DLT/LCT/C_6H_{12} solutions at the sodium D line as a function of DDT and DLT concentrations, respectively, are shown in Figure 9. The positive intercept with the *y*-axis as well as direct measurement indicate that soybean lecithin is optically active with a specific rotation $[\alpha]_D^{20}$ of +6.7° ± 0.1°. Moreover, the good linearity indicates that effects due to dimethyl tatrate concentration are negligible. Thus, the specific rotation values of DDT (+4.2° ± 0.3°) and DLT (−10.4° ± 0.6°) were derived by least-squares analysis of these experimental data. The significant difference between the absolute values of $[\alpha]_D^{20}$ suggests that the lecithin reverse micelles may possibly discriminate the two enantiomers. Moreover, it is interesting to compare these values with $[\alpha]_D^{20}$ for DDT (+15.2° ± 0.4°) and $[\alpha]_D^{20}$ for DLT (−15.8° ± 0.6°) in AOT reverse micelles, where opposite values were obtained within experimental errors.

Because the specific rotation of chiral compound in different media is influenced by the dielectric constant of the solvent and reflects solvent-induced effects on its preferential conformation(s), we compare the $[\alpha]_D$ value of DDT in lecithin reverse micelles (+4.2°) with that observed in some conventional solvents such as CCl_4 (+43.0°), DMSO (−3.1°), and water (−20.8°).[12,19]

From the comparison of these values and according to the literature, it can be argued that the polarity probed by DDT and the way of adapting its conformational states to the lecithin reverse micelles is intermediate between that in CCl_4 and DMSO.[20] Surely specific effects on the dimethyl tartrate conformations are due to its confinement in the lecithin reverse micelles.

In Figure 10, we superimpose the ECD spectra of DDT/LCT/C_6D_{12} and DLT/LCT/C_6D_{12} solutions at three *R* values and DDT in C_6H_{12} in the inset.

There is an interesting bathochromic shift of the n → π* 213 nm transition in going from the apolar solvent to the mixed DDT/LCT/C_6D_{12} (or DLT/LCT/C_6D_{12}) solutions where it happens at ca. 218 nm. As signified by optical rotation (OR) experiment, we surmise also from ECD data a special interaction of DDT(DLT) with the polar heads of lecithin, the shift being more evident at low *R*. Solvent dependence of the n → π* transition, especially regarding polar and apolar solvent, has been reported in the past.[21]

In the specific case of dimethyl tartrate, it has been demonstrated that ECD spectra are nearly solvent independent; however, the ORD data are found to be solvent dependent.[19,22] The apparent contradiction may be made acceptable if one considers that ORD can be calculated by the Kramers−Kronig transformation of the "complete" ECD spectrum, not just in the limited wavelength region accessible by commercial instruments.[19,22]

Furthermore, we plot in Figure 11, the $\Delta A = A^+ - A^-$ value for $R = 0.5$, $R = 1.5$, and $R = 1.7$ corresponding to saturation for both DDT and DLT. No difference for the two enantiomers is reported both in the values and in the linear trend of $|\Delta A|$ versus concentration. This somewhat contradicts what has been found for optical rotation. The different behavior of ECD and of OR data is parallel to what reported above for the solvent dependence of ECD and ORD data.[22]

3.3. SAXS Measurements. The scattering profiles of samples at various *R* values are shown in Figure 12.

All SAXS spectra are well-described by a model of interacting polydisperse homogeneous scattering spheres. Because small-angle X-ray scattering arises from the contrast between different adjacent domains and due to the peculiar structure of reverse micelles, the scattering centers may be considered the hydrophilic micellar cores.[23]

The parameters shown in Table 1, which may be obtained by following the fitting procedure previously described,[24] are the micellar core mean radius (r_m); the local volume fraction

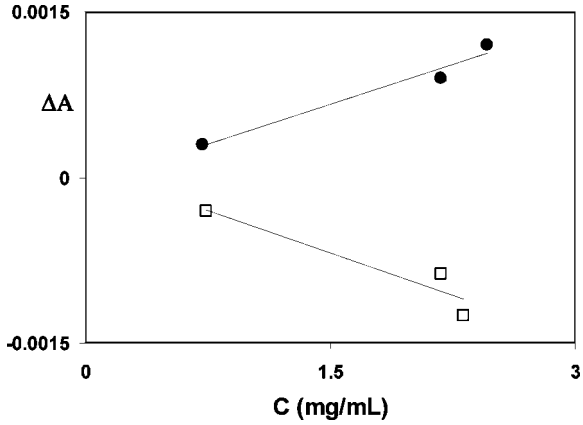

Figure 11. Observed ECD signals in $|\Delta A|$ at the maximum of the ECD band at ≈218 nm for DDT/LCT/C_6D_{12} and DLT/LCT/C_6D_{12} ([LCT] = 0.008 M) as a function of the respective enantiomers' concentrations.

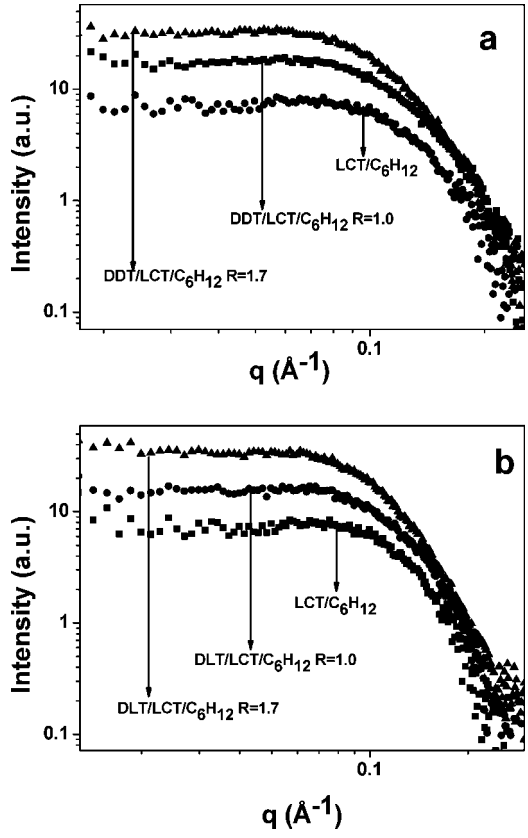

Figure 12. Scattering profiles of (a) DDT/LCT/C_6H_{12} and (b) DLT/LCT/C_6H_{12} solutions at fixed surfactant concentration ([LCT] = 0.08 M).

TABLE 1: Fitting Parameters Derived from SAXS Data Analysis of DDT/LCT/C_6H_{12} and DLT/LCT/C_6H_{12} Solutions at Fixed Surfactant Concentration ([LCT] = 0.08 M)

sample	r_m (Å)	P	Φ
LCT/C_6H_{12}	18.1 ± 0.3	0.25 ± 0.06	0.20 ± 0.06
DDT/LCT/C_6H_{12}, R = 1	18.2 ± 0.5	0.28 ± 0.05	0.18 ± 0.02
DDT/LCT/C_6H_{12}, R = 1.7	20.1 ± 0.4	0.21 ± 0.04	0.13 ± 0.05
DLT/LCT/C_6H_{12}, R = 1	18.0 ± 0.7	0.27 ± 0.06	0.17 ± 0.05
DLT/LCT/C_6H_{12}, R = 1.7	20.0 ± 0.4	0.23 ± 0.04	0.12 ± 0.02

of scattering objects (Φ), whose deviation from the mean volume fraction is a measure of the intermicellar interactions;[25] and the parameter P, which is a quantitative descriptor of the size polydispersity.

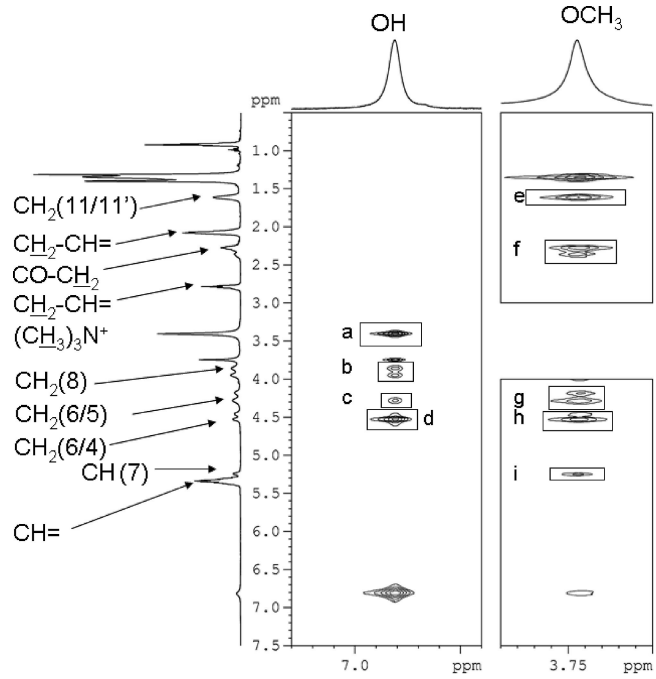

Figure 13. Expansion of NOESY spectrum of the system DDT/LCT/C_6D_{12} with R = 1.5: top trace, OH and OCH_3 signals of DDT; left trace, entire spectrum with selected assignment of lecithin protons. Framed and labeled cross peaks indicate intermolecular correlations discussed in the text. Unframed cross peaks are either diagonal peaks or intramolecular contacts. The central region corresponding to OCH_3 signal was omitted as overcrowded by its diagonal peak.

The mean micellar core radius of the dry lecithin reverse micelles obtained here (18.1 Å) can be considered in good agreement with the micellar radius previously found (25 Å) by small-angle neutron scattering technique, if the contribution given to the micellar size by the surfactant alkyl chains is accounted for.[4]

The data in Table 1 suggest that the mean micellar core radius and the polydispersity index of samples do not exhibit sizable changes with R, indicating that the micellar structure is only slightly affected by the DDT or DLT entrapment. This finding is consistent with the hypothesis that tartrates are mainly entrapped within the lecithin surfactant head groups without forming an internal micellar core.

On the other hand, the local volume fraction (Φ) of the scattering objects is greater than the volume fraction of lecithin (0.06) in the micellar solutions, thus suggesting the occurrence of intermicellar interactions leading to the formation of clusters of reverse micelles. Conversely, the decrease of Φ with increasing R indicates that a decrease of the intermicellar interactions and of the mean size of reverse micelles clusters occurs as a consequence of the tartrate encapsulation.

3.4. NMR Measurements. In previous papers the intermolecular NOE between solubilizate and surfactant was proposed as a powerful experimental tool for the assessment of the structure of reverse micelles at molecular level.[26−28]

In the present work a collection of NOESY spectra was recorded for both DDT/LCT/C_6D_{12} and DLT/LCT/C_6D_{12} systems with R = 0.5, 1.5 and 1.7. An example is reported in Figure 13. In all the experiments the observed (intra- and intermolecular) NOEs turned out to be negative (namely cross peaks in phase with diagonal peaks), thus providing a first evidence of encapsulation of tartrate diesters in a large, slowly tumbling supramolecular assembly.

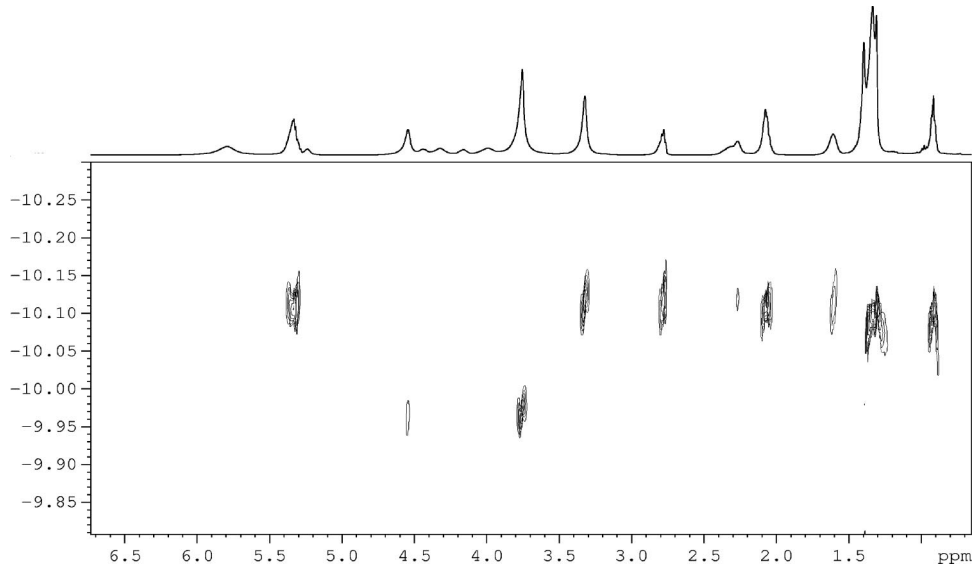

Figure 14. DOSY spectrum of the system DDT/LCT/C_6D_{12} with $R = 1.7$.

Both systems showed the same number and type of intermolecular contacts, irrespective of the absolute configuration of tartrate stereocenters. Also, the cross peaks pattern did not show relevant changes on varying *R*. These observations allow one to point out that, independently of the *R* value, both tartrate diesters share the same mode of interaction with the surfactant molecules and the same localization within the micelle. The latter fact can be derived by inspection of experimental intermolecular NOEs. The tartrate OH proton gives NOE with the protons belonging to the glycerol frame of lecithin (H atoms 6, 7, and 8; see Figure 1 for atom numbering) and with those of the choline terminal, namely CH_2 groups in positions 4 and 5 and the methyl groups of the trimethylammonium head of lecithin. The corresponding cross peaks are labeled a−d in the left part of Figure 13. The data indicate that the DDT/DLT ester is mainly located within the polar core of the reverse micelle. Three different functional groups, the phosphate, the trimethylammonium, and the ester groups, are eligible for hydrogen bond interactions with tartrate hydroxyl groups.

The OCH_3 groups of tartrate show intermolecular cross peaks with glycerol protons (CH_2 in positions 6 and 8 and CH in position 7). The corresponding cross peaks are reported in Figure 13 as g−i. In addition, strong NOE is also observed with the trimethylammonium group of choline, thus confirming the conclusions reported above. Interestingly, methoxy groups of tartrate also show correlation with some protons of the fatty acid chains. In detail, the cross peaks e and f of Figure 13 clearly indicate that the tartrate esters significantly interact with both CH_2 groups in the α and β position with respect to the carbonyl. These findings are consistent with the picture of the solubilizate molecules encapsulated within the polar core of the micelle but still able to migrate from the polar core to the boundary of the palisade. The internal dynamics of the tartrate is, however, limited to the very first CH_2 groups of the fatty acid chains: indeed, no cross peak is detectable between the OCH_3 groups of tartrate and any of the vynilic protons of the unsaturated fatty acid chains.

The formation of lecithin/D,L-tartrate aggregates, inferred from NOESY spectra was also confirmed by diffusion NMR experiments. DOSY experiments, allowing species of different effective size to be distinguished, are widely used in studying the formation of associates and guest−host complexes. Therefore a set of DOSY experiments was performed for both DDT/LCT/C_6D_{12} and DLT/LCT/C_6D_{12} systems with $R = 0.5$, 1.5 and 1.7. The 2D DOSY map for DDT/LCT/C_6D_{12} with $R = 1.7$ is shown in Figure 14.

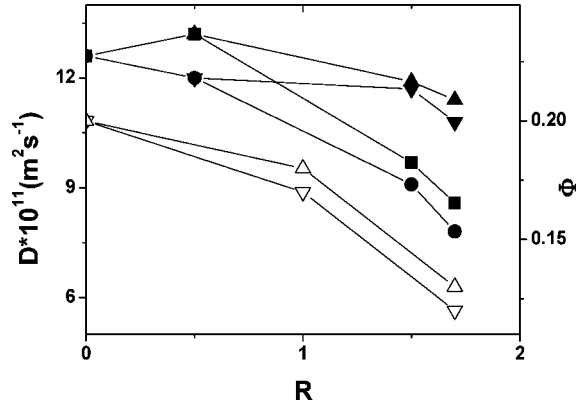

Figure 15. Diffusion coefficients of DDT, DLT, and lecithin plotted versus *R*: DDT, ▲; DLT, ▼; LCT in DDT/lecithin, ■; LCT in DLT/lecithin, ●. In the right scale, the Φ values versus *R*: DDT/LCT/C_6H_{12}, △; DLT/LCT/C_6H_{12}, ▽.

The spectrum obtained for the solution with $R = 0.5$ shows a single diffusion coefficient value corresponding to the spectral lines of both lecithin and tartrate molecules. The tartrate is entrapped in the polar core of the reverse micelles and the solubilizate−surfactant aggregates move in solution as a whole. The DOSY spectra obtained for the solutions with $R = 1.5$ and 1.7 consist of two separate peaks, one corresponding to the lecithin ^1H lines and a second one corresponding to the tartrate NMR bands. These results indicate fast chemical exchange of tartrate and lecithin molecules between different states on the NMR time scale. Interestingly, all the diffusion coefficients show the same trend with increasing *R* (e.g., all *D* values decrease with increasing *R*), but $D_{tartrate}$ are systematically slightly greater than those of the $D_{lecithin}$.

The measured diffusion coefficients for all the investigated samples are presented in Figure 15 as a function of *R*.

The interpretation of diffusion data requires a reasonable hypothesis on the processes able to sustain the molecular motions in solution of reverse micelles. In principle, three different contributions are expected for the observed diffusion coefficient of tartrate and lecithin molecules: D_{bound}, accounting

for their slow diffusion as bound species to the reverse micelles, D_{free}, referred to their diffusion as species monomerically dispersed species in the bulk solvent, and $D_{exchange}$, resulting from their fast diffusion among reverse micelle clusters. The second term (D_{free}) can be reasonably neglected, as the concentration of free tartrate and lecithin in C_6D_{12} is far below the detection limits of NMR.[29]

Thus the average observed diffusion coefficient of tartrate and lecithin molecules can be described by

$$D_{obs} = f_{exchange}D_{exchange} + f_{bound}D_{bound} \quad (1)$$

where $f_{exchange}$ and f_{bound} can be identified with the fraction of species undergoing the "exchange" and "bound" diffusion mechanism in the NMR time scale.

The existence of two main different diffusion mechanisms for both tartrate and lecithin molecules is consistent with the general picture emerging from SAXS measurements. As discussed in the previous section, the parameter Φ (the local volume fraction of scattering objects) is related to the formation of clusters of micelles and decreases with increasing R. As a consequence, also the frequency of intermicellar exchanges of tartrate and lecithin decreases. As $D_{exchange} > D_{bound}$ for both tartrate and lecithin, the decreasing trend of $D_{observed}$ with R reported in the plot can be inferred. The observed trends of D vs R and Φ vs R are then correlated. This fact is shown in Figure 15 where, for the sake of clarity, the values of the Φ parameter obtained from SAXS experiments are superimposed to those of $D_{lecithin}$ and $D_{tartrate}$ and reported onto the secondary y axis.[30,31]

4. Conclusions

Making use of spectroscopic and structural investigation methods, detailed information on the state of D and L dimethyl tartrate confined within dry lecithin reverse micelles dispersed in cyclohexane and on the resulting supramolecular aggregates has been obtained. The analysis of the spectral features of dimethyl tatrates allows us to hypothesize that both enantiomers are entrapped in the reverse micelles and, as a consequence of specific interactions, they are located in the proximity of the surfactant head groups. Also VCD and NMR spectroscopies provide clear signatures of the confinement of dimethyl tartrates within lecithin reverse micelles, thus supporting the hypothesis of specific interactions of dimethyl tartrate with polar head of lecithin. A thorough analysis of the experimental data allows us also to exclude the building up of a well-defined internal core formed by the chiral molecules even at the higher R investigated.

Apart from chiral properties, from an accurate comparison of the spectroscopic behavior of the two enantiomers, the occurrence of significant differences in these interactions has been ruled out.

We obtain strong differences in the spectroscopic absorption and VCD signals for homogeneous solutions and supramolecular aggregates in the same solvent (see in particular DDT/AOT/CCl_4 vs DDT/CCl_4) due to the fact that tartrate and surfactants build up ordered supramolecular aggregates involving several molecules as opposed to what is obtained for example in tartrate−cyclodextrin dimers.[12]

Furthermore, the similarity of the spectroscopic signals obtained for tartrate and surfactant and for tartrate and a hydrogen bond acceptor solvent like DMSO together with their interpretation through calculations, provided in ref 12, permits us to validate the picture of hydrogen bonds between tartrate and polar head groups of the surfactant.

Finally, the analysis of SAXS patterns indicates that although the DDT or DLT entrapment in the lecithin reverse micelles only slightly affects the size of micellar cores, marked changes of the intermicellar attractive interactions are induced, thus leading to a decrease of the mean size of clusters of reverse micelles with increasing R and, consequently, of the diffusion coefficients of both tartrate and lecithin.

From a more general point of view, the present investigation (based on the synergism of some selected techniques) provides a direct way to the synthesis and characterization of chiral nanostructures, thus opening the possibility of exploiting new materials with so far unexplored chiroptical properties.

Acknowledgment. Financial support from MIUR within the National Research Project "Dalle singole molecole a complessi e nanostrutture: struttura, chiralità, reattività e teoria" (PRIN 2006) is gratefully acknowledged.

Supporting Information Available: Absorption and VCD spectra in the 950−1450 cm^{-1} region (**S1**) and in the 1650−1850 cm^{-1} region (**S2**) of both enantiomers of dimethyl tartrate, DDT and DLT, in CCl_4 solution, in deuterated DMSO solution, in AOT/CCl_4 and in LCT/C_6D_{12} (for acronyms see text). In the latter two cases, we report results for one R value of the molar ratio of dimethyl tartrate to surfactant species. This information is available free of charge via the Internet at http://pubs.acs.org.

References and Notes

(1) Kumar, V. V.; Kumar, C.; Raghunathan, P. *J. Colloid Interface Sci.* **1984**, *99*, 315.
(2) Tung, S. H.; Lee, H. Y.; Raghavan, S. R *J. Am. Chem. Soc.* **2008**, *130* (27), 8813.
(3) Luisi, P. L.; Magid, L. J. *CRC Crit. Rev. Biochem.* **1986**, *20*, 409.
(4) Aliotta, F.; Fontanella, M. E.; Sacchi, M.; Vasi, C.; La Manna, G.; Turco Liveri, V. *J. Mol. Struct.* **1996**, *383*, 99.
(5) Calandra, P.; Longo, A.; Ruggirello, A.; Turco Liveri, V *J. Phys. Chem. B.* **2004**, *108*, 8260.
(6) Turco Liveri, V. *Nanosurface Chemistry*; Marcel Dekker: New York, 2001.
(7) Yu, Z. J.; Neuman, R. D. *J. Am. Chem. Soc.* **1994**, *116*, 4075.
(8) Mantegazza, F.; Degiorgio, V.; Giardini, M. E.; Price, A. L.; Steytler, D. C.; Robinson, B. H. *Langmuir* **1998**, *14*, 1.
(9) D'Aprano, A.; Donato, I. D.; Pinio, F.; Turco Liveri, V. *J. Solution Chem.* **1989**, *18*, 949.
(10) Silber, J. J.; Biasutti, A.; Abuin, E.; Lissi, E. *Adv. Colloid Interface Sci.* **1999**, *82*, 189.
(11) Ruggirello, A.; Turco Liveri, V. *J. Colloid Interface Sci.* **2003**, *258*, 123.
(12) Zhang, P.; Polavarapu, P. L. *J. Phys. Chem. A* **2007**, *111*, 858.
(13) Abbate, S.; Longhi, G.; Ruggirello, A.; Turco Liveri, V. *Colloids Surf. A: Physicochem. Eng. Aspects* **2008**, *327*, 44.
(14) Caponetti, E.; Chillura-Martino, D.; Ferrante, F.; Pedone, L.; Ruggirello, A.; Turco Liveri, V. *Langmuir* **2003**, *19*, 4913.
(15) Buffeteau, T.; Ducasse, L.; Brizard, A.; Huc, I.; Oda, R. *J. Phys. Chem. A* **2004**, *108*, 4080.
(16) Gigante, D. M. P.; Long, F.; Bodack, L. A.; Evans, J. M.; Kallmerten, J.; Nafie, L. A.; Freedman, T. B. *J. Phys. Chem. A* **1999**, *103*, 1523.
(17) Edwards, W. L.; Bush, S. F.; Mattingly, T. W.; Weisgraber, K. H. *Spectrochim. Acta Part A* **1993**, *49*, 2027.
(18) Polavarapu, P. L.; Ewig, C. S.; Chandramouly, T. *J. Am. Chem. Soc.* **1987**, *109*, 7382.
(19) Polavarapu, P. L.; Petrovic, A. G.; Zhang, P. *Chirality* **2006**, *18*, 723.
(20) Ruggirello, A.; Turco Liveri, V. *Chem. Phys.* **2003**, *288*, 187.
(21) Coulombeau, C.; Rassat, A. *Bull. Soc. Chim. Fr.* **1966**, *12*, 3752.
(22) Petroviæ, A. G. Ph.D. Thesis, Vanderbilt University, 2007.
(23) North, A. N.; Dore, J. C.; McDonald, J. A.; Robinson, B. H.; Heenan, R. K.; Howe, A. M. *Colloids Surf.* **1986**, *19*, 21.
(24) Branca, C.; Magazu, S.; Ruggirello, A.; Turco Liveri, V *J. Phys. Chem. B* **2006**, *110*, 25608.
(25) Persello, J.; Boisvert, J. P.; Guyard, A.; Cabane, B. *J. Phys. Chem. B* **2004**, *108*, 9678.

(26) Ceraulo, L.; Dormond, E.; Mele, A.; Turco Liveri, V. *Colloids Surf. A* **2003**, *218*, 255.
(27) Crans, D. C.; Rithner, C. D.; Baruah, B.; Gourley, B. L.; Levinger, N. E. *J. Am. Chem. Soc.* **2006**, *128*, 4437.
(28) Ceraulo, L.; Fanara, S.; Turco Liveri, V.; Ruggirello, A.; Panzeri, W.; Mele, A. *Colloids Surf. A* **2008**, *316*, 307.
(29) Kataoka, H.; Eguchi, T.; Masui, H.; Miyakubo, K.; Nakayama, H.; Nakamura, N. *J. Phys. Chem. B* **2003**, *107*, 12542.
(30) Walderhaug, H.; Johannessen, E. *J. Solution Chem.* **2006**, *35*, 979.
(31) Chen, A.; Wu, D.; Johnson, C. S. *J. Phys. Chem.* **1995**, *99*, 828.

JP809793U